InAlAs solar cell on a GaAs substrate employing a graded $In_xGa_{1-x}As$–InP metamorphic buffer layer

Ian Mathews' , Donagh O'Mahony, Agnieszka Gocalinska, Marina Manganaro, Emanuele Pelucchi, Michael Schmidt, Alan P. Morrison, and Brian Corbett

Citation: Appl. Phys. Lett. **102**, 033906 (2013); doi: 10.1063/1.4789521
View online: http://dx.doi.org/10.1063/1.4789521
View Table of Contents: http://aip.scitation.org/toc/apl/102/3
Published by the American Institute of Physics

InAlAs solar cell on a GaAs substrate employing a graded $In_xGa_{1-x}As$–InP metamorphic buffer layer

Ian Mathews,[1,2,a)] Donagh O'Mahony,[1] Agnieszka Gocalinska,[1] Marina Manganaro,[1] Emanuele Pelucchi,[1] Michael Schmidt,[1] Alan P. Morrison,[1,2] and Brian Corbett[1]
[1]*Tyndall National Institute, Lee Maltings, University College Cork, Cork, Ireland*
[2]*Department of Electrical and Electronic Engineering, University College Cork, Cork, Ireland*

(Received 12 October 2012; accepted 14 January 2013; published online 25 January 2013)

Single junction $In_{0.52}Al_{0.48}As$ solar cells have been grown on a (100) GaAs substrate by employing a 1 μm thick compositionally graded $In_xGa_{1-x}As$/InP metamorphic buffer layer to accommodate the 3.9% mismatch. Cells processed from the 0.8 μm thick InAlAs layers had photovoltaic conversion efficiency of 5% with an open circuit voltage of 0.72 V, short-circuit current density of 9.3 mA/cm^2, and a fill factor of 74.5% under standard air mass 1.5 illumination. The threading dislocation density was estimated to be 3×10^8 cm^{-2}. © *2013 American Institute of Physics*. [http://dx.doi.org/10.1063/1.4789521]

Currently, the state-of-the-art multi-junction solar cells (MJSC) have an efficiency of 43.5%[1] under concentration. The recent improvement in efficiency of MJSCs has been achieved through the use of alloys for the junctions, which have lattice constants mismatched to the substrate as these provide better bandgap combinations to split the solar spectrum. Metamorphic growth techniques provide compositionally graded buffer layers where the dislocations caused by strain are effectively confined to the graded layers.[2,3] These cells are based on alloys with lattice parameters near that of GaAs, which limit the ultimate performance. Recently,[4] it has been highlighted that a move to a multi-junction system based on a lattice parameter close to that of InP would offer greater potential for increasing the overall cell efficiency. The growth and fabrication of an $In_{0.52}Al_{0.48}As$ solar cell lattice matched to an InP substrate has been reported with an 1-Sun efficiency of 14%,[5] which has been further extended to an InAlAs/InGaAsP/InGaAs triple-junction structure also lattice-matched to InP.[6] In order to further develop the feasibility of this material system for commercial multi-junction device production, there is a need to consider alternatives to the InP substrate given its cost, maximum available substrate diameter, and mechanical robustness, in particular when compared with GaAs, Ge, or Si.

In this Letter, we demonstrate the realisation of an $In_{0.52}Al_{0.48}As$ solar cell on a GaAs substrate where a metamorphic buffer layer (MBL) based on superlinearly graded $In_xGa_{1-x}As$ compositions is used to alter the lattice constant from the GaAs host substrate of 5.65 Å to that of 5.87 Å (InP). We compare the electro-optic characteristics of $In_{0.52}Al_{0.48}As$ cells grown on GaAs with those grown lattice-matched on an InP substrate. An efficiency of 5% for a 0.63 mm^2 cell on GaAs is measured under 1-Sun illumination. The cell on the InP substrate under a metal shading of 5% has a projected efficiency of 14.67%.

The InGaAs MBL was grown on a perfectly oriented (100) GaAs wafer by metal organic vapour phase epitaxy (MOVPE) in an Aixtron 200 MOVPE reactor. The growth was performed with standard hydride and metalorganic trimethyl-III sources, at 80 mbar, with nitrogen as carrier gas, disilane and de-ethyl zinc as doping sources. The substrate temperature, as confirmed by an optical pyrometer, was set at 650 °C during the growth of GaAs and decreased with increasing In inclusion in the graded structure to 620 °C for the InP cap layer. The grading of the GaAs lattice constant to that of InP was performed over a thickness of 1 μm, by growing $In_xGa_{1-x}As$ up to a value of x = 53% indium using one parabolic[7] and two linear grading regions, as illustrated in Fig. 1, in a similar way to that reported for grading from InP to InAs,[8] although without employing surfactants effects. The MBL was characterised using high resolution X-ray diffraction (HRXRD) reciprocal space mapping. Based on Vegard's law, the parallel strain[9] for the InP cap layer on the MBL was estimated to be ≈−1.8%, which corresponds to an in-plane lattice parameter of 5.8686 Å.

The InAlAs solar cell structure was then grown in a second stage on the MBL on GaAs. An n-type InP substrate

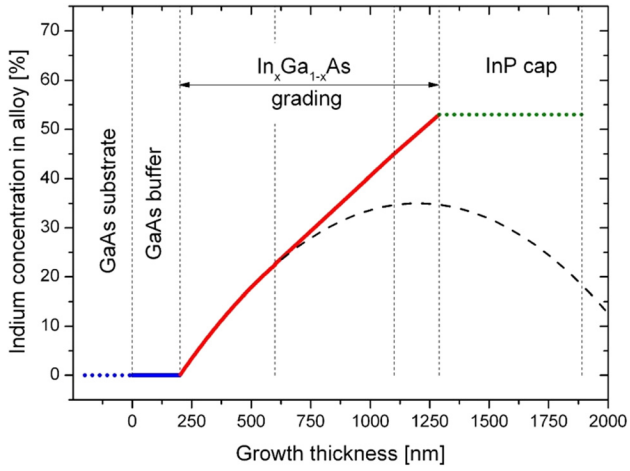

FIG. 1. Overview of the metamorphic buffer layer growth profile. The homoepitaxial buffer GaAs layer is followed by alloys of a continuous convex compositional gradient of the In content from x = 0% to 53%. The grading comprises of three sections: first 400 nm along a parabolic curve, then linearly, with the slope of the curve reduced for the final 190 nm. The structure is capped with an InP layer, grown under our best established growth conditions as in Ref. 10.

a)Electronic mail: ian.mathews@tyndall.ie.

((100), 0.5° towards ⟨111⟩, 1×10^{18} cm^{-3}) was included in the growth run for reference. Following de-oxidation at 740 °C for 15 min, the cell structure was grown at a fixed substrate temperature of 640 °C, and the V/III ratio and growth rate were maintained at approximately 110 and 1 μm/h, respectively, for the InAlAs layers. The layer structure is as follows: first, a highly doped 2 μm thick n-type (5×10^{18} cm^{-3}) InP layer was grown to provide a low resistance lateral conduction layer for contacting to the n-type region of the cell since the graded layers are nominally un-doped. This was followed by an 800 nm thick absorbing region employing $In_{0.52}Al_{0.48}As$ n-type (4×10^{17} cm^{-3}) base and p-type (3×10^{18} cm^{-3}) emitter layers. A thin (20 nm) strained p-type wide-bandgap $In_{0.35}Al_{0.65}As$ window layer was then grown as an electron blocking front-surface field window layer. This has been previously shown to reduce surface recombination velocity in single-junction $In_{0.52}Al_{0.48}As$ solar cells while maintaining high photocurrents as the thin layer of wider bandgap material results in low parasitic absorption.[5] Finally, a highly p-doped (2×10^{19} cm^{-3}) $In_{0.53}Ga_{0.47}As$ cap layer was grown to reduce the resistance of the front contact. A schematic cross-section of the structure is shown in Fig. 2. The wafer structure was characterised by transmission electron microscopy (TEM), HRXRD, and electrochemical capacitance-voltage profiling to confirm layer thickness, crystal quality, and doping profile.

Fig. 3 shows a cross-sectional TEM image of the MBL substrate illustrating the initially highly defective region near the GaAs surface (A1). The various grading layers are visible in the image and the defective region appears to be mostly limited to the first (parabolic grading) layer, labelled A2 in Fig. 3, where strain effects are greatest. In general, defects are seen to propagate laterally in this first graded layer (A2) rather than threading vertically towards the upper layers of the MBL where they would impact on the quality of the solar cell structure. Nevertheless, some defects are still visible in the InP capping layer (A5) at the surface of the MBL, which may lead to structural defects in the solar cell layers.

Figure 4 presents HRXRD measurements of the solar cell structure grown on the MBL substrate referenced to the (004) diffraction angle of GaAs. The position of the layer peak with respect to the substrate ($\Delta 2\theta = -1.358°$) indicates an InP/InAlAs lattice constant with strain of about −1.8%,

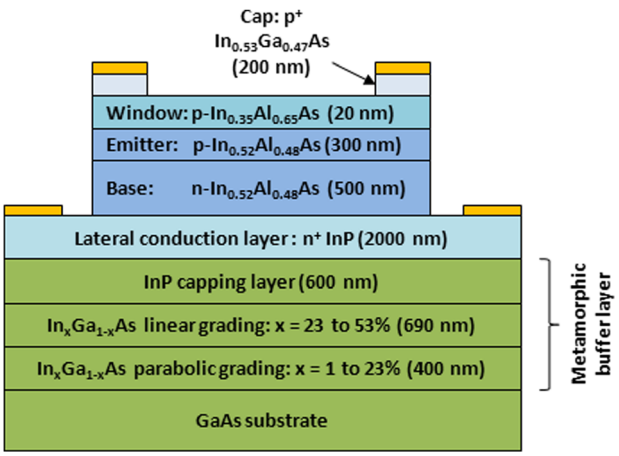

FIG. 2. Schematic cross section of the InAlAs solar cell grown on the metamorphic buffer on a GaAs substrate.

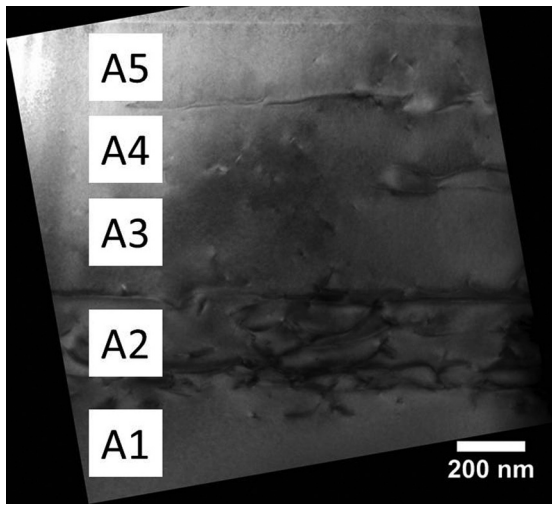

FIG. 3. Cross-sectional bright field TEM image of the MBL of the solar cell structure. (A1) GaAs substrate; (A2) 400 nm $In_xGa_{1-x}As$ parabolic grading from 1 to 23% indium; (A3) and (A4) 690 nm $In_xGa_{1-x}As$ linear grading 23% to 53%; (A5) 600 nm InP capping layer.

similar to that measured for the MBL before growth of the solar cell layers.

The diffraction width along the Omega axis is seen to broaden from that of the relatively narrow signal associated with the GaAs substrate (FWHM = 0.0136°) through the MBL structure to that of the solar cell layers (FWHM = 1.141°), which can be correlated with the defective nature of the MBL substrate as evidenced by the TEM image of Fig. 3. A shoulder at lower angles is also evident on the main InAlAs/InP peak, indicating a mismatch between some of the grown layers, possibly due to the InGaAs cap layer. A lower intensity diffraction signal is also evident at an intermediate angle between the substrate and main InAlAs/InP layer peaks, which is most likely due to the thin (20 nm) highly strained InAlAs window with ~65% Al content.

Solar cells (area = 0.63 mm^2, metal grid coverage = 24%) were fabricated with p-contact (Ti/Pt/Au, 30/50/300 nm) and n-contact (Au/Ge/Au/Ni/Au, 14/14/14/11/250 nm), selective H_3PO_4:H_2O_2:H_2O based wet etching of the $In_{0.52}Al_{0.48}As$ layers to define a mesa structure and

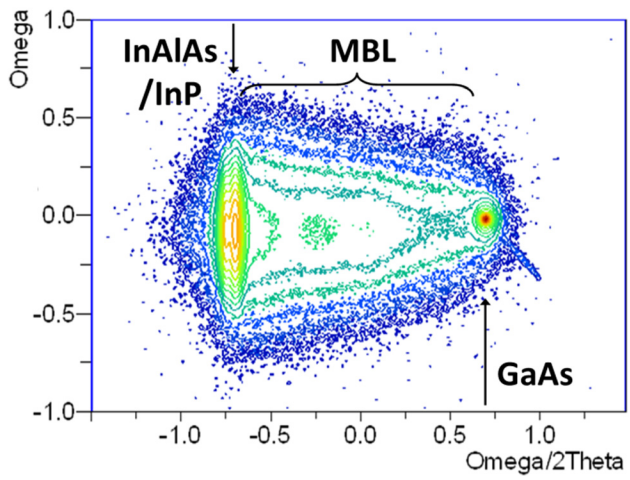

FIG. 4. 2-axis X-ray diffractogram of the InAlAs solar cell structure grown on the MBL substrate illustrating diffraction from the GaAs substrate, the metamorphic buffer layers (MBL), and the InAlAs/InP solar cell structure.

$C_6H_8O_7$:H_2O_2 selective etch to remove the absorbing $In_{0.53}Ga_{0.47}As$ cap layer in the window region. A 70 nm thick film of SiN was deposited on the front surface of the cells to provide a single-layer anti-reflection coating and to passivate the mesa sidewalls. The SiN layer was opened over the contact busbars by dry etching to allow electrical probing of the cells. For comparison, circular mesa diodes (diameter = 1 mm, metal coverage = 48%) were fabricated on the n-type InP substrates using the same process except the n-type contact covered the backside of the substrate.

The forward and reverse biased dark current density–voltage (J-V) characteristics of the cells on both substrates were measured from 20 °C to 200 °C as shown in Fig. 5. At 20 °C in forward bias with V < 0.8 V, the cells grown on the InP substrate are dominated by a diode ideality, n, of n ~ 2 corresponding to non-radiative Shockley-Read-Hall (SRH) recombination in the depletion region of the diode. Both the associated reverse saturation current (J_{SRH}) and the leakage current at V = −0.4 V have a thermal activation energy of roughly half the InAlAs bandgap also corresponding to n ~ 2. For V > 0.8 V, the ideality drops reaching 1.6 at V = 1.1 V corresponding to increasing contribution of diffusion current.

In forward bias, the cells grown on the MBL are also dominated by n ~ 2 (n = 2.2 at 0.8 V) but with J_{SRH} higher by a factor of 100 at 20 °C compared with the cells on InP. This factor reduces to 5 at 200 °C. At low forward bias (V < 0.5 V at 20 °C), there is an additional temperature dependent shunt resistance contributing to the current (see inset to Fig. 5). At higher biases, the SRH current dominates. This resistive component also dominates the current under reverse bias where it has an activation energy of ~100 meV. At higher temperatures (>140 °C), the forward current is dominated by an ideality of 1.8 and 1.6 for cells on the MBL and on InP, respectively.

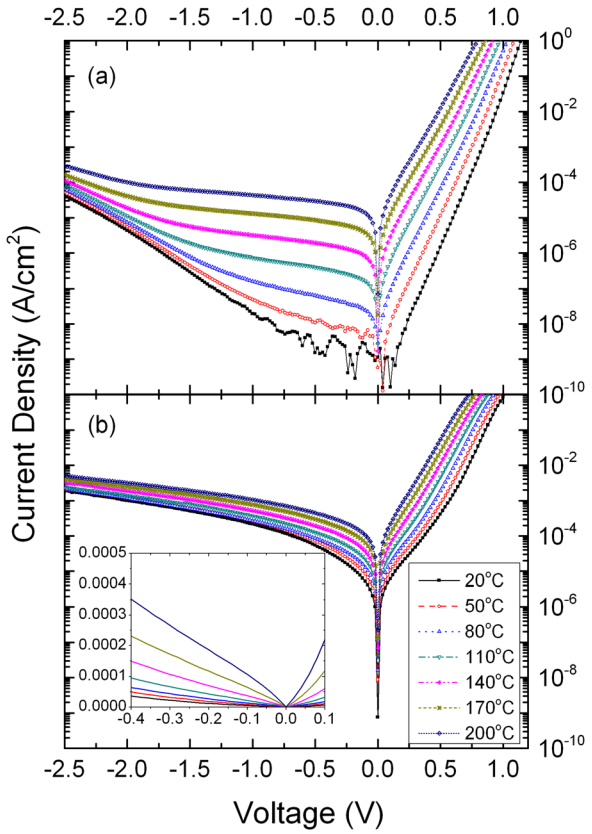

FIG. 5. Current density vs voltage characteristics as a function of temperature for InAlAs diodes on (a) InP substrate and (b) MBL/GaAs substrates. The inset to (b) plots the data on a linear scale around V = 0 V.

The SRH reverse saturation current can be expressed as in Eq. (1), where $n_i(T)$ is the temperature dependent intrinsic carrier concentration, W_d is the depletion depth, and $\tau(T)$ is the minority (hole) carrier lifetime. At 20 °C, τ values of 12 ns and 0.122 ns are extracted for the cells on InP and MBL, respectively.

$$J_{SRH} = \frac{qn_i(T)W_d}{2\tau(T)}. \quad (1)$$

It has been shown previously[11] that SRH currents in III-V solar cells can be correlated with the threading dislocation density (TDD) in the junction. A shorter minority carrier lifetime increases the reverse saturation current and reduces the open circuit voltage of a solar cell. An estimate of the TDD in the MBL structure can be found by analyzing the dark J-V characteristics of the devices.[12] Eq. (2) expresses contributions to the total lifetime, τ_{total}, from the defect free dopant dependent minority carrier lifetime, τ_{max}, and τ_{TDD} the contribution from the TDs where D is the minority-carrier diffusion co-efficient

$$\frac{1}{\tau_{Total}} = \frac{1}{\tau_{max}} + \frac{1}{\tau_{TDD}} = \frac{1}{\tau_{max}} + \frac{\pi^3(D)(TDD)}{4}. \quad (2)$$

Using the minority-carrier lifetime extracted above, the TD contribution to the minority-carrier diffusion length is calculated to be 0.124 ns. The Hall mobility of an n-doped base layer (370 nm, 3.7×10^{17} cm^{-3}) grown on a semi-insulating InP substrate was measured to be 1410 cm^2/V s yielding a diffusion co-efficient of 36 cm^2/s for electrons. The hole diffusion coefficient is estimated to be 3.6 cm^2/s based on the ratio of effective masses for electrons and holes being 0.1 (Ref. 12) from which an estimated TDD of 3×10^8 cm^{-2} is obtained.

The photovoltaic conversion efficiency was measured using a Newport Oriel 92123 series 1600W solar simulator where the incident spectrum was calibrated at 0.1 W/cm^2 using a reference cell (Fig. 6). The diodes on the InP substrate achieved an open-circuit voltage of 925 mV, a fill factor (FF) of 79%, a short-circuit current density of 9 mA/cm^2, leading to a photovoltaic conversion efficiency of 6.6%. The cell structure on the MBL substrate with a lower percentage metal shading, produced a higher short-circuit current density of 9.3 mA/cm^2, an open-circuit voltage of 724 mV, and efficiency of 5% while maintaining a high FF of 75%. The low photocurrent response of the control mesas on the InP substrate is due to the 48% shading loss. The drop in open-circuit voltage can be attributed to reduced lifetimes on the MBL structure, which are a factor of 100 lower than the InP substrate.

The measured and fitted[13] EQE curves are presented in Fig. 7. The derived hole minority-carrier lifetimes were used to simulate the response along with the measured diffusion

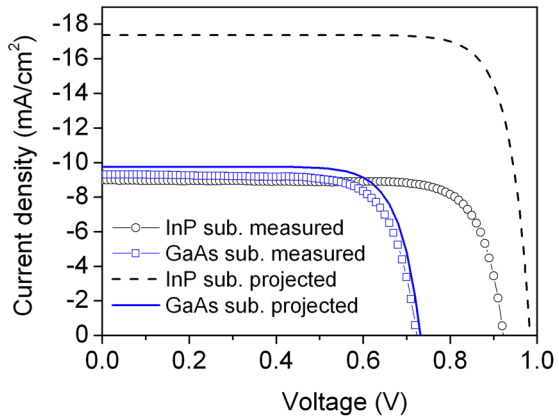

FIG. 6. Measured current density–voltage characteristics of the InAlAs devices on InP and GaAs substrates under 1-Sun illumination. Projected performance for large area solar cells is given for both substrate types.

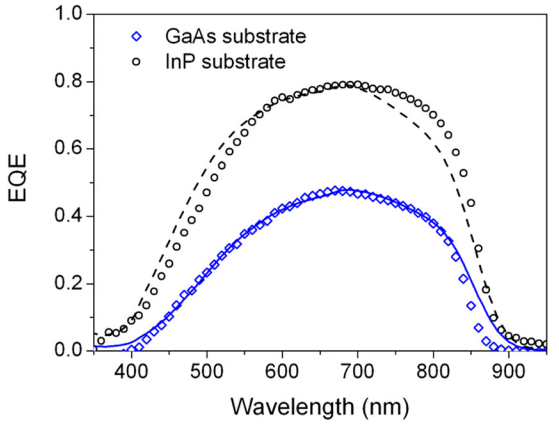

FIG. 7. External quantum efficiency as measured for both the InAlAs solar cells grown on the GaAs substrate (diamonds) and mesa diodes on the InP substrate (circles). The simulated responses are given as a straight (GaAs) and dashed line (InP).

coefficients, absorption, and reflection values. The diffusion lengths used in the presented simulations are 0.7 μm and 2 μm in the emitter and base regions of cells on the InP substrate with significantly decreased values of 180 nm and 280 nm in the corresponding regions for cells on the MBL. The modelled front surface recombination velocities increase significantly from the InP to the MBL substrates from 2×10^4 cm/s and 2.5×10^6 cm/s, respectively.

From the experimental data, it is possible to calculate a projected photovoltaic performance under the AM1.5 G spectrum to correct for the high shading loss in the devices.[14] The method assumes the dark current of the diodes is representative of larger area solar cells and calculates the expected short-circuit current density of cells using the measured EQE, and the reference standard ASTM G173-03 AM1.5 G spectrum where a 5% shading loss for large area cells is assumed. The projected photovoltaic performance is presented in Table I. The projected short-circuit density of cells on lattice matched InP substrates with a 0.8 μm thick absorbing layer is 17.3 mA/cm^2 with a 1-Sun efficiency of 14.67%.

TABLE I. Projected AM1.5G photovoltaic performance for $In_{0.52}Al_{0.48}As$ solar cells on InP and GaAs substrates.

	J_{sc} (mA/cm^2)	V_{oc} (V)	FF (%)	Efficiency (%)
InP substrate	17.3	0.986	85.6	14.67
GaAs substrate	9.8	0.734	80.7	5.79

In summary, we have demonstrated the concept of an InAlAs solar cell grown on a GaAs substrate with an InGaAs/InP metamorphic buffer layer. The device combines a solar cell with a lattice constant of InP to a GaAs host substrate and had a measured photovoltaic conversion efficiency of 5% under 1-Sun illumination. Further work is required to improve the MBL quality in order to achieve comparable efficiency with devices on bulk InP substrates. Nevertheless, the result offers a route to developing multi-junction solar cell devices based on a lattice parameter near that of InP, thus extending the range of available bandgaps for high efficiency cells.

The authors acknowledge the financial support of Enterprise Ireland, the European Regional Development fund through Grant No. TD/08/338 for the project MODCON-PV, the Irish Higher Education Authority Program for Research in Third Level Institutions (2007-2011) via the INSPIRE programme and Science Foundation Ireland through Grant Nos. 09/SIRG/I1621, 10/IN.1/I3000, and 07/SRC/I117. The authors are grateful to Dr. K. Thomas for his MOVPE system support.

[1]M. A. Green, K. Emery, Y. Hishikawa, W. Warta, and E. D. Dunlop, Prog. Photovolt **20**, 12 (2012).
[2]J. F. Geisz, D. J. Friedman, J. S. Ward, A. Duda, W. J. Olavarria, T. E. Moriarty, J. T. Kiehl, M. J. Romero, A. G. Norman, and K. M. Jones, Appl. Phys. Lett. **93**, 123505 (2008).
[3]S. Wojtczuk, P. Chiu, X. Zhang, D. Derkacs, C. Harris, D. Pulver, and M. Timmons, in *Proceedings of the 35th IEEE Photovoltaic Specialists Conference* (Honululu, Hawaii, 2010), pp. 001259–001264.
[4]R. J. Walters, M. Gonzalez, J. G. Tischler, M. P. Lumb, J. R. Meyer, I. Vurgaftman, J. Abell, M. K. Yakes, N. Ekins-Daukes, J. G. J. Adams, N. Chan, P. Stavrinou, and P. P. Jenkins, in *2011 37th IEEE Photovoltaic Specialists Conference (PVSC)* (2011), pp. 000122–000126.
[5]M. S. Leite, R. L. Woo, W. D. Hong, D. C. Law, and H. A. Atwater, Appl. Phys. Lett. **98**, 093502 (2011).
[6]R. L. Woo, W. D. Hong, S. Mesropian, M. S. Leite, H. A. Atwater, and D. C. Law, in *Proceedings of the 37th IEEE Photovoltaic Specialists Conference* (IEEE, Seattle, Washington, 2011).
[7]B. H. Müller, R. Lantier, L. Sorba, S. Heun, S. Rubini, M. Lazzarino, A. Franciosi, E. Napolitani, F. Romanato, A. V. Drigo, L. Lazzarini, and G. Salviati, J. Appl. Phys. **85**, 8160 (1999).
[8]A. Gocalinska, M. Manganaro, and E. Pelucchi, Appl. Phys. Lett. **100**, 152112 (2012).
[9]J. Sass, K. Mazur, F. Eichhorn, W. Strupiński, A. Turos, and N. Schell, J. Alloys Compd. **401**, 249 (2005).
[10]A. Gocalinska, M. Manganaro, E. Pelucchi, and D. D. Vvedensky, Phys. Rev. B **86**, 165307 (2012).
[11]J. C. Zolper and A. M. Barnett, IEEE Trans. Electron Devices **37**, 478 (1990).
[12]C. L. Andre, D. M. Wilt, A. J. Pitera, M. L. Lee, E. A. Fitzgerald, and S. A. Ringel, J. Appl. Phys. **98**, 014502 (2005).
[13]X. Lu, S. Huang, M. B. Diaz, N. Kotulak, R. Hao, R. Opila, and A. Barnett, IEEE J. Photovolt. **2**, 214 (2012).
[14]N. J. Ekins-Daukes, K. W. J. Barnham, J. P. Connolly, J. S. Roberts, J. C. Clark, G. Hill, and M. Mazzer, Appl. Phys. Lett. **75**, 4195 (1999).